



**Cloud-microphysical
sensors
intercomparison at
the Puy-de-Dôme
Observatory, France**

G. Guyot et al.

**Cloud-microphysical sensors
intercomparison at the Puy-de-Dôme
Observatory, France**

**G. Guyot¹, C. Gourbeyre¹, G. Febvre¹, V. Shcherbakov^{1,4}, F. Burnet²,
J. C. Dupont³, K. Sellegri¹, and O. Jourdan¹**

¹Laboratoire de Météorologie Physique, Université Blaise Pascal, Clermont-Ferrand, France

²CNRM/GAME – Météo-France/CNRS, 42 avenue Gaspard Coriolis, 31057 Toulouse, France

³Institut Pierre-Simon Laplace, Université Versailles Saint Quentin, 78280 Guyancourt, France

⁴Laboratoire de Météorologie Physique, Institut Universitaire de Technologie d'Allier, Montluçon, France

Received: 18 March 2015 – Accepted: 6 May 2015 – Published: 3 June 2015

Correspondence to: O. Jourdan (o.jourdan@opgc.univ-bpclermont.fr)

Published by Copernicus Publications on behalf of the European Geosciences Union.

Title Page

Abstract

Introduction

Conclusions

References

Tables

Figures



Back

Close

Full Screen / Esc

Printer-friendly Version

Interactive Discussion



Abstract

Clouds play an important role on the radiative budget of the earth (Boucher et al., 2013). Since the late 70s, several instrumental developments have been made in order to quantify the microphysical and optical properties of clouds, for both airborne and ground-based applications. However, the cloud properties derived from these different instrumentations have rarely been compared.

In this work, we discuss the results of an intercomparison campaign, performed at the Puy de Dôme during May 2013. During this campaign, a unique set of cloud instruments were compared. Two Particle Volume Monitors (PVM-100), a Forward Scattering Spectrometer Probe (FSSP), a Fog Monitor (FM-100) and a Present Weather Detector (PWD) were sampling on the roof of the station. Within a wind tunnel located underneath the roof, two Cloud Droplet Probes (CDP) and a modified FSSP (SPP-100) were operating. The main objectives of this paper are to study the effects of wind direction and speed on ground based cloud observations, to quantify the cloud parameters discrepancies observed by the different instruments, and to develop methods to improve the quantification of the measurements.

The results reveal that all instruments, except one PVM, show a good agreement in their sizing abilities, both in term of amplitudes and variability. However, some of them, especially the FM-100, the FSSP and the SPP, display large discrepancies in their capability to assess the cloud droplet number concentrations. As a result, the total liquid water content can differ by up to a factor of 5 between the probes. The use of a standardization procedure, based on data of integrating probes (PVM-100 or visibilimeter) and extinction coefficient comparison, substantially enhances the instrumental agreement. During the intercomparison campaign, the total concentration agreed in variations with the visibilimeter, except for the FSSP, so corrective factor can be applied and range from 0.43 to 2.2. This intercomparison study highlights the necessity to have an instrument which provides a bulk measurement of cloud microphysical or optical properties during cloud ground-based campaigns. Moreover, we show that the orienta-

AMTD

8, 5511–5563, 2015

Cloud-microphysical sensors intercomparison at the Puy-de-Dôme Observatory, France

G. Guyot et al.

Title Page

Abstract

Introduction

Conclusions

References

Tables

Figures

◀

▶

◀

▶

Back

Close

Full Screen / Esc

Printer-friendly Version

Interactive Discussion

tion of the probes in the main wind flow is essential for an accurate characterization of cloud microphysical properties. In particular, FSSP experiments show strong discrepancies when the wind speed is lower than 3 ms^{-1} and/or when the angle between the wind direction and the orientation of the instruments is greater than 30° . An inadequate orientation of the FSSP towards the wind direction leads to an underestimation of the measured effective diameter.

1 Introduction

The cloud droplet size distribution is one of the key parameter for a quantitative microphysical description of clouds (Pruppacher and Klett, 1997). It plays an important role in the radiative characteristics of clouds and, for example, is needed to assess the anthropogenic influence on the size and number of cloud droplets (Twomey, 1974, 1977) and on the cloud lifetime (Albrecht, 1989). Moreover, the knowledge of droplet size distribution is crucial for a better understanding of the onset of precipitation (Kenneth and Ochs, 1993) and the aerosol-cloud interaction (McFarquhar et al., 2011). According to Brenguier et al. (2003), aerosol-cloud interaction studies need accurate assessment of the cloud microphysical properties such as liquid water content (LWC), concentration and effective diameter. Moreover, the representation of liquid stratiform clouds in current climate models is relatively poor, leading to large uncertainties in climate predictions (Randall et al., 2007). Radiative, dynamic and feedback processes involved in liquid clouds still need to be studied (e.g., Petters et al., 2012; Bennartz et al., 2013) and thus require accurate measurement instrumentation. In addition, in situ measurements may be directly used for model validations, or to improve and validate remote sensing, RADAR and LIDAR retrieval algorithms.

A large set of instruments have been developed since the late 70's to obtain precise information on cloud microphysical and optical properties. Two strategies are mainly used to measure in situ properties of clouds. The first one consists in mounting instruments under the wings of an aircraft that flies within the cloud (Gayet et al., 2009;

AMTD

8, 5511–5563, 2015

Cloud-microphysical sensors intercomparison at the Puy-de-Dôme Observatory, France

G. Guyot et al.

Title Page

Abstract

Introduction

Conclusions

References

Tables

Figures

◀

▶

◀

▶

Back

Close

Full Screen / Esc

Printer-friendly Version

Interactive Discussion



Cloud-microphysical sensors intercomparison at the Puy-de-Dôme Observatory, France

G. Guyot et al.

Baumgardner et al., 2011; Brenguier et al., 2013). The other one consists in instruments operated on a ground-based platform, generally on a mountain site, which altitude allows sampling natural clouds (Kamphus et al., 2010). The main measurement principle for the size detection used in most of these devices is based on a conversion of the forward scattering of light into a size bin using the Lorentz–Mie theory (Mie, 1908). However, comparisons between the various devices reveal large discrepancies (Baumgardner, 1983; Burnet and Brenguier, 1999, 2002). In addition, when the same method is employed, previous studies showed that some effects could influence the measurements, e.g., Gerber et al. (1999) highlighted the inertial concentration effect and Wendisch et al. (1998) highlighted activity corrections, changing velocity acceptance ratio, wind ramming effect, Mie curve adjustment and sensitivities to droplet size and concentration. A cloud ground based experiment performed at the Junfraujoch, Switzerland, by Spiegel et al. (2012), showed potential biases in the absolute values of the parameters, especially comparing the Fog Monitor to others instruments. Burnet and Brenguier (2002) also pointed out noticeable differences in fog measurements for airborne instrumentation, where a maximum of 30 % biases were found for the LWC. Then, as recommended for airborne measurements in Brenguier et al. (2013), it is still of crucial importance to perform liquid water cloud instrumental comparison with ground based experiments.

The site of the Puy de Dôme, France, provides a unique opportunity for an intercomparison study of cloud microphysical measurements. Indeed, the station is in clouds about 50 % on the time on average (annual mean). The station consists of a platform on the roof, where a ground-based instrumentation can be installed, and a wind tunnel facing the dominant western winds used to sample air masses at air speeds up to 55 ms^{-1} in order to reproduce airborne conditions. In this paper, we will focus on the cloud instrumentation intercomparison performed within the ROSEA (Réseau d’Observatoires pour la Surveillance et l’Exploration de l’Atmosphère, i.e., Network of Monitoring centers for the Study and the Supervision of the Water Atmospheric). The first objective is to provide a status of the instrumental variability within the cloud micro-

Title Page

Abstract

Introduction

Conclusions

References

Tables

Figures

◀

▶

◀

▶

Back

Close

Full Screen / Esc

Printer-friendly Version

Interactive Discussion



2014), aerosol hygroscopic properties (Asmi et al., 2012; Holmgren et al., 2014), cloud chemistry (Marinoni et al., 2004; Deguillaume et al., 2014) and cloud microphysics (Mertes et al., 2001).

The ROSEA intercomparison campaign took place from 16 to 28 May 2013 (see Table 1 for the details). Eleven cloudy episodes were sampled, each for several hours. Temperatures were always positive, thus preventing freezing from affecting the measurements. The meteorological situation was characterized by westerly winds with speeds ranging from 1 to 22 ms⁻¹. The cloud microphysical properties evidenced values of droplet effective diameter ranging between 10 and 30 μm and liquid water content (LWC) values were between 0.1 and 1 gm⁻³.

2.2 Cloud instrumentation and sampling methodology

During the ROSEA campaign, a set of instruments was deployed on the PUY station sampling platform and in the wind tunnel to provide a description of cloud droplets with diameters ranging from a few to 50 μm. Measurements include particle size distribution, effective diameter, extinction coefficient, LWC and number concentration. The set of instruments mounted on the roof terrace was composed of a Forward Scattering Spectrometer Probe (PMS FSSP-100), a Fog Monitor (DMT FM-100), two PVM-100 (Particle Volume Monitor) GERBERs and a PWD (Present Weather Detector) (see Fig. 1a).

The Forward Scattering Spectrometer Probe (FSSP-100) initially manufactured by Particle Measuring Systems, Inc. of Boulder, Colorado is the oldest instrument still in use for measuring cloud droplet size distribution. The FSSP counts and sizes each droplet individually from an aspirated airstream, using forward (between the angles 4° and 12°) scattered laser-light intensity ($\lambda = 0.633 \mu\text{m}$) and the Mie theory, to compute the droplets size (Knollenberg, 1981). The operation, the accuracy, the limitations and the corrections are detailed by Dye and Baumgardner (1984), Baumgardner et al. (1985) and Baumgardner and Spowart (1990). For water droplet clouds, the accuracy of the derived effective diameter and LWC was estimated as 2 μm and 30 %,

Cloud-microphysical sensors intercomparison at the Puy-de-Dôme Observatory, France

G. Guyot et al.

Title Page

Abstract

Introduction

Conclusions

References

Tables

Figures

◀

▶

◀

▶

Back

Close

Full Screen / Esc

Printer-friendly Version

Interactive Discussion



respectively (Febvre et al., 2012). According to Gayet et al. (1996), errors in particle concentration can reach 20 to 30 %. In the operating range used at the PUY, the resulting counts were summarized into 15 size bins, each of 3 μm width, beginning from 2 μm and ending at 47 μm of the diameter. LWC was calculated by integrating the droplet volumes from the measured droplet spectrum and dividing the total mass of liquid water by the sampled air volume. The theoretical air speed through the inlet was 9 ms^{-1} . The FSSP was checked periodically to keep the inlet facing into the wind.

The total concentration N , LWC and extinction coefficient σ are respectively computed using the following equations (Cerni, 1983):

$$N[\text{cm}^{-3}] = \sum_D \frac{n(D)}{S \cdot \text{TAS} \cdot \Delta t} \quad (1)$$

$$\text{LWC} [\text{gm}^{-3}] = \frac{\pi}{6} \times 10^{-6} \cdot \sum_D n(D) D^3 \quad (2)$$

$$\sigma[\text{km}^{-1}] = \frac{\pi}{2} \cdot \sum_D n(D) D^2 \quad (3)$$

where $n(D)$ is the concentration measured for the size class of diameter D , TAS the speed of the air in the inlet (True Air Speed) and Δt the sampling duration. S is the sampling surface computed as the Depth of Field (DOF) multiplied by the width of the laser beam. The equation of the extinction coefficient takes into account the approximation that the extinction efficiency is equal to 2 within the droplet size and laser wavelength range. These equations are also valid for the FM 100 and the CDP. The activity correction and changing Velocity Acceptance Ratio (VAR) (Wendisch, 1998) were taken into account in the calculations. The activity correction consists of a factor, lower than 1, applied to Δt in order to account for the losses due to instrument dead time. The changing VAR stems from the fact that only part of the laser beam diameter is used to calculate the sampling volume because drops passing the laser beam near its edges are undersized. The others effects will be discussed below.

Cloud-microphysical sensors intercomparison at the Puy-de-Dôme Observatory, France

G. Guyot et al.

Title Page

Abstract

Introduction

Conclusions

References

Tables

Figures

◀

▶

◀

▶

Back

Close

Full Screen / Esc

Printer-friendly Version

Interactive Discussion



Cloud-microphysical sensors intercomparison at the Puy-de-Dôme Observatory, France

G. Guyot et al.

The Fog monitor (FM-100) is a forward scattering spectrometer probe ($\lambda = 0.658 \mu\text{m}$) placed in his own wind tunnel with active ventilation (Eugster et al., 2006), manufactured by Droplet Measurement Technologies, Inc., Boulder, USA, designed for use during ground-based studies. This instrument measures the number size distribution of cloud particles (with a high time resolution) in the size range between 2 and $50 \mu\text{m}$. For the ROSEA experiments, we used a resolution of 20 channels describing the size distribution. Details about the operation of this instrument are given by Droplet Measurement Technologies (2011). According to Spiegel et al. (2012), uncertainties in concentration resulting from particle losses, i.e. sampling losses and losses within the FM-100 can be as high as 100 %. The FM-100 was installed on the mast next to the FSSP.

The Particle Volume Monitor (PVM-100, manufactured by Gerber Scientific, Inc., Reston, Virginia) is a ground-based forward scattering laser spectrometer for particulate volume measurements (Gerber, 1984, 1991). It is designed to measure the LWC, the particle surface area (PSA) and to derive the droplet effective radius (r_{eff}). The PVM-100 measures the laser light ($\lambda = 0.780 \mu\text{m}$) scattered in the forward direction by an ensemble of cloud droplets which crosses the probe's sampling volume of 3cm^3 . The light scattered in the 0.25 to 5.2° angle range is collected by a system of lenses and directed through two spatial filters. The first filter converts scattered light to a signal proportional to the particle volume density (or LWC) of droplets; the second filter produces a signal proportional to the particle surface area density (PSA) (Gerber et al., 1994). From the ratio of these two quantities, r_{eff} is derived. These two filters guarantee a linear relationship between scattering intensity and LWC or PSA for droplets diameter from 3 to $45 \mu\text{m}$ for the PVM-100 (Gerber, 1991). The extinction coefficient σ is directly proportional to the PSA. According to Gerber et al. (1994), the accuracy of LWC is 10 % for this diameter range. The airborne version of the PVM is the PVM-100A which has a different set of filters to enhance sampling volume resulting in a reduced sensitivity to larger droplets. Gerber et al. (1994) showed that the PVM-100A response to atomized droplets underestimates LWC by 18 % for a median volume diameter (MVD) of $30 \mu\text{m}$,

Title Page

Abstract

Introduction

Conclusions

References

Tables

Figures

◀

▶

◀

▶

Back

Close

Full Screen / Esc

Printer-friendly Version

Interactive Discussion



Cloud-microphysical sensors intercomparison at the Puy-de-Dôme Observatory, France

G. Guyot et al.

Title Page

Abstract

Introduction

Conclusions

References

Tables

Figures

◀

▶

◀

▶

Back

Close

Full Screen / Esc

Printer-friendly Version

Interactive Discussion

et al. (2001). During the campaign a forward scattering spectrometer probe SPP-100 model and two Cloud Droplet Probes (CDP) were installed in the sampling section of the wind tunnel (see Fig. 1b) to characterize the cloud microphysical properties in terms of droplet size distributions and extinction coefficients. Four experiments were performed in the wind tunnel, each with the duration of nearly two hours (see Table 1).

The SPP-100 is a modified model of the FSSP-100 (manufactured by Droplet Measurement Technologies DMT, Inc., Boulder, USA) with 40 size classes and a revised signal-processing package (fast-response electronic components). Brenguier et al. (2011) have shown that the SSP-100 noticeably improve the accuracy of the size distribution assessment compare to the FSSP-100 version.

The CDP is a forward-scattering optical spectrometer ($\lambda = 0.658 \mu\text{m}$), manufactured by DMT. Light scattered by a particle is collected over a range of angles from 4 to 12° in the forward direction and then split equally between the qualifier and sizer, which allow the instrument to count and size the cloud droplets. According to Lance et al. (2010), oversizing of 60% and undercounting of 50% can occur in the CDP due to coincidence. Mie resonance structure is most pronounced for a single mode laser such as used in the CDP (Lance et al., 2010), while a multi-mode laser, as is used in the standard FSSP, can potentially dampen the Mie resonances (Knollenberg et al., 1976). As a consequence, some size bins were grouped to a total of 24 size bins, instead of 30 initially, from 3 to 49 μm . The two CDPs were installed in the wind tunnel.

During the campaign, measurements were performed with 1 Hz acquisition frequency instruments. Data have been averaged over ten seconds or one minute, depending on the duration of the experiment, and cloud heterogeneity, possible small gap in time synchronization of the instruments and eventual high variability of the measurements. The PVM1 measurements are provided with routine protocol which averaged the data over 5 min, thus any comparison with this instrument has to be carried out with 5 min average data. The FSSP show incoherent measurement from 23 to 26 March, probably due to electronic interferences. An overview of the data availability during the campaign is shown in Table 2.

3 Results

3.1 Data analysis strategy based on a preliminary case study

The purpose of this section is to give an overview of the microphysical measurement strategy performed during the campaign with a focus on the instrument variability. During the 16 May a large number of instruments were deployed simultaneously on the station platform and in the wind tunnel (see Table 1).

Figure 2 provides an example of the temporal evolution of the parameters measured the 16 May. On this graph, we choose to represent only the time series of the cloud properties when the wind tunnel was actually in function, the data are averaged over 10 s. The wind speed outside and inside the wind tunnel is shown in Fig. 2a. The outside wind speed varied from 2 to 7 m s⁻¹ while the air speed in the wind tunnel was set up to fixed values ranging from 25 to 55 m s⁻¹. The measured cloud parameters display in Fig. 2b–d are: the effective diameter, the number concentration and the liquid water content of cloud droplets measured by the FSSP, the PVM 2 (except for the concentration) and the FM on the roof of the PdD station as well as those ones obtained from the two CDP and the SPP located in the wind tunnel. The time series of the extinction coefficient derived from these instruments and the PWD are shown in Fig. 2e. The observed cloud layers were above the freezing level with temperatures almost constant around 1 °C. During the sampling period, the dominant wind was blowing westward and the instruments positioned on the mast were oriented accordingly.

Both the values and the variability of the effective diameter measured by the instruments are in good agreement with a correlation coefficient close to 0.9 (Fig. 2b). Only one instrument is an exception, strong discrepancies are observed when comparing the effective diameter of the PVM2 to the others instruments. As the discrepancies of the PVM2 can only be explained by a dysfunction of the instrument, its results were not further discussed.

The temporal evolution of the number concentration exhibit systematic differences among the instruments (Fig. 2c) although the microphysical properties variability is

AMTD

8, 5511–5563, 2015

Cloud-microphysical sensors intercomparison at the Puy-de-Dôme Observatory, France

G. Guyot et al.

Title Page

Abstract

Introduction

Conclusions

References

Tables

Figures

◀

▶

◀

▶

Back

Close

Full Screen / Esc

Printer-friendly Version

Interactive Discussion



Cloud-microphysical sensors intercomparison at the Puy-de-Dôme Observatory, France

G. Guyot et al.

well captured by all the instruments (correlation coefficient close to 0.9). The number concentration measured by the FM 100 is systematically lower than that one derived from the other instruments whereas the FSSPs (SPP and FSSP-100) show the highest values. The ratio of concentration (namely the FSSP number concentration divided by the FM number concentration) derived from these two types of instruments reaches values up to 5. As for the CDPs installed in the wind tunnel, the concentration measurements lie between the values obtained by the FSSPs and the FM 100. The cloud droplet concentrations measured by the two CDP instruments vary up to a factor of 2, and by a factor of 1.3 (CDP1) and 2.2 (CDP2) compared with cloud droplet concentrations measured by the FSSP. Similarly, the LWC and extinction coefficient values show significant discrepancies. The bias between the instruments is potentially very important (up to 5 when comparing the FSSPs concentration to the FM 100). However, the temporal variability of the data are well correlated (R^2 close to 0.9).

This example illustrates that the probes adequate sizing of cloud droplets is subject to a systematic bias when particle counting (number concentration) is involved. This can be clearly seen in Fig. 3 where the average Particle Size Distributions (PSD) measured by the different spectrometer probes are displayed.

The PSD show similar trends and shapes, with modes from 10 to 14 μm which explains the agreement in the effective diameter values. The computed average Mean Volume Diameter (MVD) shows similar values with a maximum deviation of 1.3 μm , which is within the instrumental errors. This confirms the good agreement observed between all the instruments in the qualitative parameters. However, the discrepancies observed for the magnitude (concentration) of the PSD are significant and linked to the systematic concentration bias evidenced in Fig. 2. This means that the size bins partitioning is correct and the number concentration discrepancies are likely to come from an incorrect assessment of the probe sampling volume. In addition, the SPP-100 tends to overestimation the number concentration for the largest particles (larger than 30 μm), compared to the other instruments, especially for the two CDPs of the wind tunnel. One of possible explanations could be the effect of splashing artifacts inside

Title Page

Abstract

Introduction

Conclusions

References

Tables

Figures

◀

▶

◀

▶

Back

Close

Full Screen / Esc

Printer-friendly Version

Interactive Discussion



the SPP inlet, as evidenced by Rogers et al. (2006). This result highlights the difficulties to accurately derive the droplets concentration, which was expected due to the lack of simple number calibration for these instruments.

The red-framed parts of the time series displayed in Fig. 2 correspond to additional experiments where the orientation of the instruments on the mast was changed (the FM 100 and the FSSP). Those orientation changes lead to a strong decrease of all the microphysics parameters of the instruments installed on the mast, especially of the FSSP. The data corresponding to those orientation experiments are removed for the following analysis and will be discussed in the Sect. 3.4. On the example of 16 May, we observe that the differences in concentrations measured with different probes seem to vary, and may be a function of wind speed and direction. As a consequence, in Sect. 3.2, we compare instruments in the next section over the entire campaign when they all were orientated coaxially to the wind direction.

Concerning the wind tunnel, the experiments highlight the effect of the air speed applied to the measurements. Figure 4 shows the evolution of the 10 s average size distribution of the two CDPs present in the wind tunnel, during the experiment of the 16 May. During this day, the air speed in the wind tunnel varies between 25 and 55 m s^{-1} , but the abrupt variations in air speed have no effects on the size distributions of both CDP1 and CDP2. This result is applicable to the entire campaign. The air speed has to be taken into account in the calculation of the sampling volume and the total droplet concentration. However, through comparisons with cloud droplet distributions measured on the roof and in the wind tunnel we confirm that the sampling of the cloud performed in the wind tunnel does not modify its microphysical properties.

3.2 Instrumental intercomparison for wind-isoaxial conditions

In this section, we focus on measurements performed in the wind tunnel and on the roof of station when the wind was isoaxial to the sampling probes inlets, over the whole campaign. Microphysical changes, due to the orientation of the instruments, observed in Fig. 2, will be investigated in Sect. 3.4. The data are averaged over 10 s for the

Cloud-microphysical sensors intercomparison at the Puy-de-Dôme Observatory, France

G. Guyot et al.

Title Page

Abstract

Introduction

Conclusions

References

Tables

Figures

◀

▶

◀

▶

Back

Close

Full Screen / Esc

Printer-friendly Version

Interactive Discussion



wind tunnel measurements and over 1 min for ambient conditions in order to make the measurements comparable (see Sect. 2.3).

Figure 5 displays the scatter plots of the effective diameter for the instruments deployed on the PUY platform. There is a good agreement between the FM 100 and the FSSP as confirmed by the high linear correlation coefficient value ($R^2 = 0.94$). Additionally, the bias observed between these two instruments is within the “theoretical” measurement errors. The comparison between the PVM1 and the FSSP and FM-100 shows that the overall variability of cloud droplet effective diameter is well captured (R^2 close to 0.9). Even if the slope of the linear regression is greater than 1, the measurement points are close to the line 1 : 1 and the scatter is within the measurement uncertainties. Such discrepancy between the FM100 and the PVM has already been reported in Burnet and Brenguier (2002) and analyses are currently conducted to better understand such behavior. Moreover, the comparisons (not shown here) between the PVM 1 and the FM 100 extinction and LWC give a slope a of 2.1 with $R^2 = 0.72$ and $a = 2.6$ with $R^2 = 0.78$ respectively. When comparing the PVM 1 and the FSSP 100 the slopes are $a = 0.35$ with $R^2 = 0.65$ and $a = 0.4$ with $R^2 = 0.8$ for the extinction and the LWC respectively. The rather good correlations obtained between the instruments as well as the comparable slope for the extinction and the LWC can be explained by the agreement of the effective diameter for the different instruments. The bias between these instruments results from a constant error originating from the inaccurate assessment of the sampling volume or the number calibration coefficient.

The comparison between the number concentrations measured coaxially to the wind direction by the FSSP and the FM-100 over the whole campaign is displayed in Fig. 6. The concentration measurements are slightly less correlated than the effective diameter measurements but the correlation remains acceptable ($R^2 = 0.79$). However, a significant discrepancy (slope of 0.15 which corresponds to a factor 6) between the instrument concentration measurements is clearly evidenced. This ratio of 6 is the same as that one obtained when LWC are compared (not shown), thus confirming that the sizing

Cloud-microphysical sensors intercomparison at the Puy-de-Dôme Observatory, France

G. Guyot et al.

Title Page

Abstract

Introduction

Conclusions

References

Tables

Figures

◀

▶

◀

▶

Back

Close

Full Screen / Esc

Printer-friendly Version

Interactive Discussion

is coherent between the two instruments. The constant bias found for the concentration affects the extinction and the LWC in the same way.

Moreover the effect of the wind speed on the concentration measurements is color coded in Fig. 6. We can observe that the measurements performed under low wind speed conditions (lower than 5 ms^{-1}) are more scattered compared to the ones corresponding to higher wind speed. We will discuss this point in details, specifically concerning the FSSP data, in Sect. 4.

Figure 7 shows the comparison between the 5 min averaged extinction coefficients measured by the PVM 1 and the PWD, two instruments that do not need active ventilation. There is a good agreement between the two instruments ($R^2 = 0.86$) and the slope is close to 1. The small discrepancies between these two instruments can be attributed to the heterogeneity of the cloud properties and instrumental errors. The points with the low extinction values show larger variations, corresponding to the cloud edge where the properties are the most heterogeneous. However, the Pearson Principal Component Analysis (see Pearson et al., 1901, for details) shows that the correlation remains significant.

Therefore, the fact that there is a systematic constant bias (slope of 6 in Fig. 6) in the intercomparison of the droplet number concentration and of the LWC measured by the different probes, could be indicative of the inaccurate assessment of the probe sampling volume directly linked to the air flow speed measurement accuracy. In order to discuss this issue, the measurements performed under ambient conditions can be compared with the measurements in the wind tunnel where the air flow is accurately monitored.

During the campaign a forward scattering spectrometer probe SPP-100 model and two CDPs were installed in the sampling section of the wind tunnel (see photo 2). Four wind tunnel experiments were performed with a varying applied wind tunnel air speed from 10 to 55 m s^{-1} (see Table 2 for details).

Figure 8a presents the results of the effective diameter as the intercomparisons for the three instruments installed in the wind tunnel. Good agreement is observed among

AMTD

8, 5511–5563, 2015

Cloud-microphysical sensors intercomparison at the Puy-de-Dôme Observatory, France

G. Guyot et al.

Title Page

Abstract

Introduction

Conclusions

References

Tables

Figures

◀

▶

◀

▶

Back

Close

Full Screen / Esc

Printer-friendly Version

Interactive Discussion

all the probes, with correlation coefficients R^2 always larger than 0.9. The slope of the linear regression is close to 1, meaning that the assessment of this parameter is consistent for the CDPs and the SPP-100 thus confirming the good calibration in diameter.

The measured droplet concentrations comparisons, presented in Fig. 8b, also show high correlation coefficients ($R^2 = 0.9$), comparable to those measured for the effective diameter. However, linear regression analysis shows that the slopes vary between 0.42 and 0.69 for the different instruments. It should be noted that these slopes are independent of the air speed applied in the wind tunnel. Even though, the discrepancies are less pronounced than those ones for the instruments placed on the platform of the PdD station, a significant bias still exists (up to a factor of 2). This bias may be attributed to the assessment of the probe sampling speed/volume. In particular, it is known that the Depth Of Field (DOF) of an instrument can be significantly different from the value given by the manufacturer. This uncertainty may exceed a factor 2 (Burnet and Brenguier, 2002) and can thus explain a large part of the biases observed between the instruments in terms of concentration, extinction and LWC.

In order to evaluate the consistency of measurements performed in ambient air (on the mast) with those performed in a wind controlled environment, we can characterize the relative sensitivity of the droplet concentration measurements to the wind speeds. As already discussed, all the instruments in the wind tunnel are very well correlated. Since only the slope of the linear regression differs from one instrument to another, we choose to compare the FSSP and the FM 100 sampling on the roof, with the SPP100 sampling in the wind tunnel. These instruments are based on the same measurement principle.

Figure 9 displays the scatter plots of the number concentration measured by the instruments on the mast against the SPP observations performed during the four wind tunnel experiments (the 16, 22, 24 and 28 May with the 10 s average measurements). The concentrations measured by the FM-100 are rather well correlated to the SPP observations even though the wind speeds are quite different for the instruments on

Cloud-microphysical sensors intercomparison at the Puy-de-Dôme Observatory, France

G. Guyot et al.

Title Page

Abstract

Introduction

Conclusions

References

Tables

Figures

◀

▶

◀

▶

Back

Close

Full Screen / Esc

Printer-friendly Version

Interactive Discussion



measurements as well as on the study of the effect of the air speed (wind speed or suction in the wind tunnel) on the measurements.

3.3 Improvement of data processing

The difficulties to estimate the speed of cloud particles inside the inlets, which directly impacts the assessment of the sampling volume value and derived quantities such as the number concentration, combined with the fact that there is no number calibration for the instrumentation lead to the need to standardize the recorded data. The most natural way is to standardize the measurements with instruments which are not based on single particle counting but on the measurements of an ensemble of particles (i.e. from an integrated value). Such measurements are performed by the PVM-100 and the PWD.

Since good agreement was found between the extinction coefficients measured by the PVM 1 and the PWD (Fig. 7), these two instruments can be used as absolute reference of the extinction of cloud particles. As the PWD was the only instrument working during the entire campaign, all recorded data are standardized according to this instrument. Hence, the data of other instruments were averaged over 1 min according to the PWD time resolution.

Figure 10 presents the comparison between one minute averaged PWD extinctions and the data obtained in the wind tunnel for all the experiments, as a function of the wind tunnel air speed. The results show good correlations ($R^2 > 0.7$), and the slope of the regression curves corresponds to the correction coefficient applied to the sampling volume of the probes. The dispersion can be attributed to the spatial difference between the instruments on the roof and in the wind tunnel and the instrumental errors. The factors of 0.44 and 0.63 were found, respectively for the SPP and the CDP 1. As those coefficients are linked to the modification of the sampling volume and number calibration, they can be applied to the concentration, the extinction and the LWC with a simple relation of proportionality. Moreover, as discussed in Sect. 3.1, and shown in Fig. 10, air speed in the wind tunnel has no influence on the measured data when the

Cloud-microphysical sensors intercomparison at the Puy-de-Dôme Observatory, France

G. Guyot et al.

Title Page

Abstract

Introduction

Conclusions

References

Tables

Figures

◀

▶

◀

▶

Back

Close

Full Screen / Esc

Printer-friendly Version

Interactive Discussion



Cloud-microphysical sensors intercomparison at the Puy-de-Dôme Observatory, France

G. Guyot et al.

Title Page

Abstract

Introduction

Conclusions

References

Tables

Figures

◀

▶

◀

▶

Back

Close

Full Screen / Esc

Printer-friendly Version

Interactive Discussion



sampling volume correction is taken into account. This agrees with the results obtained for the 16 May and shown in Fig. 4. The measurements performed with an air speed equal to 10 ms^{-1} were removed from the dataset because of the high discrepancies observed with the PWD observations ($R^2 = 0$ for the SPP and 0.4 for the CDP 1), meaning that the sampling is inadequate at this speed. For cloud measurements, we thus recommend to use the wind tunnel with an air speed higher than 10 ms^{-1} .

In a similar way Fig. 11 presents the comparison of the PWD extinctions with the instruments placed on the mast during the campaign, as a function of the external wind speed (right panels). The FM 100 and PWD measurements are correlated, even though the FM 100 extinction is underestimated by a factor 2 compared to the PWD reference measurements. This factor is of the same order of magnitude as the bias found when comparing the PWD to the instruments positioned in the wind tunnel (Fig. 10). On the other hand, Fig. 11 shows only a poor correlation between the FSSP and the PWD extinction coefficient measurements. Additionally, the wind speed seems to have an influence on the FSSP measurements. Several points, corresponding to low wind speeds, show a large overestimation of the extinction measured by the FSSP. Removing the data corresponding to a wind speed lower than 5 ms^{-1} , leads to a better correlation ($R^2 = 0.55$) and a slope of 0.4. It should be pointed out that the results remain almost unchanged for the FM 100 when removing the same low wind speed cases. As a consequence, the FSSP seems to be very sensitive to meteorological conditions, especially the wind conditions. Again, this reveals that low wind speeds contribute heavily towards the amount of scatters so that some physical phenomenon seems to affect the droplet detection (see Sect. 4).

Table 3 presents the summary of the instrumental intercomparison during the ROSEA campaign in term of the instrumental bias (slope a) and the correlation coefficient R^2 . In this Table, the correlation between two instruments has been computed when the data of the two instruments were available at the same time (see Table 2), with coaxial measurements toward the wind direction, and during stable cloudy periods. One minute averaged data were used to compare the instruments on the roof

Cloud-microphysical sensors intercomparison at the Puy-de-Dôme Observatory, France

G. Guyot et al.

Title Page

Abstract

Introduction

Conclusions

References

Tables

Figures

◀

▶

◀

▶

Back

Close

Full Screen / Esc

Printer-friendly Version

Interactive Discussion



while. Ten seconds averaged data were used to compare instruments when wind tunnel instrumentation is involved. However, due to the time resolution (see Table 1), comparison with the PWD is made at 1 min average and with the PVM1 at 5 min average. The comparisons between the PVM1 and the wind tunnel instruments are not representative due to the lack of points. Comparisons with the PWD measurements, colored in orange, give the coefficient to be applied in order to normalize the data of each instrument. All the instruments, except the FSSP, show at least an acceptable correlation ($R^2 \geq 0.6$) with the PWD during the entire campaign, independently of the meteorological conditions.

Up to now we have investigated the coherence of performed measurements using the different probes sampling isoaxially to the main wind stream. In the following section, we will investigate the effect of non-isoaxial sampling on the measurements.

3.4 Effect of wind direction

In this section we focus on experiments where the mast was orientated in different directions with respect to the main wind stream. Each position was maintained during 5 min and the orientation was regularly moved back and forth to an isoaxial position to check if the cloud properties remained unchanged during the experiment. Four measurement series were carried out during 22 May. The wind was blowing west all day long and the cloud properties were rather stable.

Figure 12 presents the temporal evolution of the FSSP and FM 100 size distributions along with the wind speed and the deviation angle between the instrument orientation and the wind direction. First, for the measurement with an angle equal to 0° , the cloud size distribution is almost unchanged throughout the experiment. The FSSP LWC and number concentration are approximately 1 gm^{-3} and 1000 cm^{-3} , respectively. Notable changes are observed from angles of 30° . The concentration decreases with increasing angles and with a more pronounced impact for large water droplets (larger than $15 \mu\text{m}$ approximately). An impact on the small droplets is also seen for large angles, but appears to be lower for low wind speeds. Indeed, comparing the series 3 and 4

with the average values of wind speed of 7 and 3 ms⁻¹, the size distribution shows a higher decrease in concentration when the wind is strong. The FM 100 shows the same behavior but with a lower sensitivity.

The impact of the combination of both wind speed and direction on the probe's efficiency to sample cloud droplets is clearly illustrated in Fig. 13, which shows the cloud droplet size distribution, averaged for each angle θ and average wind speed. The percentage of the FSSP isoaxial number concentration loss for each angle and wind speed values is shown in Table 4. This percentage is computed for the total size range of droplets, for small and for large droplets, arbitrarily defined as a droplet diameter lower or greater than 14 μm respectively. On average, the greater the angular deviation from isoaxial configuration is, the more the size distribution is reduced, except for a 3 ms⁻¹ wind speed. For wind speed 5, 6 and 7 ms⁻¹, the total percentages displayed on Table 4 go up from 74, 75 and 28 % to 95, 96 and 98 %, respectively. The results also show that, for the same angle of deviation, the percentage increases with increasing wind speed, with only one exception for 30° and a wind speed of 7 ms⁻¹. Thus, with increasing wind speed, the total percentage goes up from 88 to 93 % for 60° and from 95 to 98 % for 90°.

However for a wind speed of approximately 3 ms⁻¹, the size distribution shows very small changes. Despite a ratio of about 4 between the coaxial and a deviation angle of 60°, the size distribution displays the same shape whatever the angle is. Indeed, the particle loss percentages presented on Table 4 for small and the large droplets, show very small differences compared to the other wind speed values. The size distribution could then be corrected by applying a constant factor. However, for wind speeds higher than 5 ms⁻¹, the FSSP size distribution shape changes, the effective diameter decreases, if the instrument is not facing the wind. Table 4 shows that the particle loss percentage for small particles is almost always lower than for larger droplets. This means that the reduction of the measured particle number concentrations resulting from changes in instrument orientation is more efficient for large particles. An inadequate orientation of the mast leads to an underestimation of the effective diame-

Cloud-microphysical sensors intercomparison at the Puy-de-Dôme Observatory, France

G. Guyot et al.

Title Page

Abstract

Introduction

Conclusions

References

Tables

Figures

◀

▶

◀

▶

Back

Close

Full Screen / Esc

Printer-friendly Version

Interactive Discussion

ter. Therefore, a simple correction of the size distribution is not possible if the wind is greater than 3 m s^{-1} and the deviation angle is larger than 30° .

Table 5 shows the results for the FM 100. For the same wind speed and direction, the values of the FM 100 concentration loss are systematically lower than for the FSSP.

This means that the FM 100 undergoes a weaker loss of measured particles when the instruments are not facing the wind. The variations of the FM 100 concentration loss with the wind speed and the angle are less obvious than of the FSSP. Moreover, the amplitude of these variations is much weaker than for the FSSP, with a minimum of 15% and a maximum of 68%. This confirms that the FM 100 is less sensitive to the wind speed and orientation than the FSSP-100.

4 Discussion

In order to further investigate the influence of the wind speed on the FSSP response, three additional experiments with the SPP-100 installed on the mast along with the FSSP were performed (from the 13 to the 15 November 2013).

The SPP has an internal estimation of the droplet speed within the sampling volume: the so-called transit speed. We recall that ideally the transit speed through the laser beam should be the same as the SPP sampling speed. In addition, this also allows us to estimate the values and the variations of the sampling volume, needed in the computation of the concentration, when assuming that the air speed is close to the particle speed. The SPP was connected to the pump used with an aspiration speed of 15 m s^{-1} which corresponds to a theoretical sampling speed in the instrument's inlet of 9 m s^{-1} . The instruments on the mast were always oriented to assure coaxial measurements. The goal of this study was to use the SPP transit speed measurements to quantify the FSSP sampling volume as a function of the wind speed and the pump aspiration speed, in order to have a better understanding of the sampling processes in the inlets.

Over the period of 13 to 15 November, the wind speeds ranged from 0 to 15 m s^{-1} and LWC values varied between 0 and 1 g m^{-3} . The SPP transit time showed rela-

AMTD

8, 5511–5563, 2015

Cloud-microphysical sensors intercomparison at the Puy-de-Dôme Observatory, France

G. Guyot et al.

Title Page

Abstract

Introduction

Conclusions

References

Tables

Figures

◀

▶

◀

▶

Back

Close

Full Screen / Esc

Printer-friendly Version

Interactive Discussion



Cloud-microphysical sensors intercomparison at the Puy-de-Dôme Observatory, France

G. Guyot et al.

Title Page

Abstract

Introduction

Conclusions

References

Tables

Figures

◀

▶

◀

▶

Back

Close

Full Screen / Esc

Printer-friendly Version

Interactive Discussion

tively high variations between 7 and 12 μs . Transit time is theoretically inversely proportional to transit speed. These values correspond to SPP transit speeds between 15 and 25 m s^{-1} , which are higher than the theoretical value of 9 m s^{-1} that was taken into account for the data processing of both the SPP and the FSSP. Even if the transit speed depends on the particle size distribution, these differences could explain the overestimation of the concentration and the LWC obtained from the FSSP data. It emphasizes the need of an accurate estimation of the sampling volume. Indeed, an error on the determination of the DOF or the air speed, combined with the absence of the number calibration coefficient, lead to potentially high biases even if the instruments are still capable to capture the cloud properties variations.

In order to explain the variations of the SPP transit time, it can be compared to the wind speed and the pumping speed. Figure 14 presents the comparisons of one minute averaged data. The effective diameter measured by the SPP is also shown on the colorbar. It should be pointed out that the effective diameter values higher than 20 μm were observed only during a relatively small period of time when the wind speed was below 7 m s^{-1} . The transit time fluctuates independently of the wind speed or of the pump aspiration. As a consequence, there is no simple explanation to describe the absolute values and the variations of the SPP transit time.

Choularton et al. (1986) compared the FSSP volume sampling rate V to wind speed values. In that experiment, the ground-based FSSP was coupled with a fan with a sampling speed of 26 m s^{-1} , which corresponds to a value of $V = 8.14 \text{ cm}^3 \text{ s}^{-1}$ in windless air conditions. The wind speed varied approximately between 10 and 20 m s^{-1} . The measured FSSP volume sampling rate V increased from 12 to 16 $\text{cm}^3 \text{ s}^{-1}$ with increasing wind speed. Such values correspond to the sampling speed from 38 to 51 m s^{-1} . Choularton et al. (1986) concluded that the ventilation speed and hence the volume sampling rate is modified by the forcing of air through the sample tube by the wind, known as the ramming effect.

This ramming effect was not observed during our November 2013 experiments. First, the sampling air speed within the FSSP inlet was higher than expected (≥ 15 instead

Cloud-microphysical sensors intercomparison at the Puy-de-Dôme Observatory, France

G. Guyot et al.

Title Page	
Abstract	Introduction
Conclusions	References
Tables	Figures
◀	▶
◀	▶
Back	Close
Full Screen / Esc	
Printer-friendly Version	
Interactive Discussion	

of 9 ms^{-1}). This difference can be attributed to the underestimation of the diameter value of the instrument's laser beam (that value was set at manufacture). The results of Fig. 14 show that the ramming effect cannot explain the overestimation of the concentration of the FSSP and SPP or the relatively high variability of the SPP transit time. At the same time, the variability observed in the SPP transit time measurements explains the variations in number concentrations when compared to the PWD (Figs. 10 and 11). The assumption that the SPP and the FSSP have the same behavior in ground based conditions and the high variability in the FSSP sampling speed leads to high uncertainties in computed number concentrations and extinctions. That is why the FSSP number concentration and extinction show high discrepancies with the SPP and the CDP 1 (both installed in the wind tunnel) and the PWD (mounted on the roof terrace) measurements.

In addition, the variability seems to be a function of the droplet diameter. Indeed, for a diameter lower than $20 \mu\text{m}$, the SPP transit speed varies approximately between 12 and 27 ms^{-1} whereas, for a diameter greater than $20 \mu\text{m}$, the SPP transit speed is between 15 and 20 ms^{-1} . In the non-isokinetic conditions and for high Reynolds number (about 2×10^4), turbulent flows are expected inside and near the FSSP inlet. This could lead to strong changes in the droplets trajectories and speeds. The smaller the particle is, the more it follows the air flows. This explains why smallest droplets have the highest variability in the SPP transit speed. This result highlights the complex influence and importance that air flow and droplet inertia may play in the measurements.

Gerber et al. (1999) compared the LWC measurements of the FSSP and the PVM-100 during ground-based experiments. This study highlighted the need of the knowledge of the ambient wind speed and the instrument orientation with respect to the wind direction, and suggested that the FSSP overestimates the concentration due to the droplet trajectories inside the flow accelerator when the ambient air speed is inferior to the velocity near the position of the laser. A simple trajectory model was used to understand if the suction used to draw droplets into the sampling tube of the FSSP can cause changes in the droplet concentration at the point where the laser beam inter-



Cloud-microphysical sensors intercomparison at the Puy-de-Dôme Observatory, France

G. Guyot et al.

Title Page

Abstract

Introduction

Conclusions

References

Tables

Figures

◀

▶

◀

▶

Back

Close

Full Screen / Esc

Printer-friendly Version

Interactive Discussion

acts with the droplets. The modeling was performed for a sampling velocity of 25 m s^{-1} and two wind-speed values of 0 and 2 m s^{-1} . As expected, the air flow converges and accelerates into the inlet. At the same time, droplets are unable to follow the curved streamlines and, due to the droplets' inertia, show a tendency to accumulate near the centerline of the insert where the sampling volume is located. The overestimation can be determined by the enhancement factor F given by the ratio of FSSP concentration near the centerline of the insert to the ambient concentration. The enhancement factor decreases with increasing wind speed (from 0 to 2 m s^{-1}) and increases with increasing droplet effective radius (from 0 to $25 \mu\text{m}$). For a droplet radius of $25 \mu\text{m}$, the concentration enhancement varies between a factor of 3.5 and 30 depending on the ambient air velocity. For droplet smaller than $R_{\text{eff}} = 5 \mu\text{m}$ the enhancement is less than 10%. FSSP is behaving as an inertial droplet concentrator that generates spurious droplet concentration much larger than ambient values. Errors are small for droplet radius less than $5 \mu\text{m}$ but increases rapidly with increasing droplet size.

To compare our results with Gerber et al. (1999) findings, Fig. 15 displays the ratio between the FSSP and PWD extinctions as a function of the effective radius provided by the FSSP and the wind speed, for the entire ROSEA campaign. The lowest values of the PWD extinction were removed in order to avoid unrealistic ratio values. The ratio of extinction or LWC (used in Gerber et al. (1999)) is the same within the hypothesis that it is due to an inaccurate assessment of the sampling volume. As we selected the PWD as the reference instrument, this ratio is similar to the enhancement factor F from Gerber et al. (1999). Our results show high values and variability of the ratio for low values of the wind speed whereas the ratio is constant (~ 2.5 which join the slope of 0.4 seen in the Fig. 11) when the wind speed is greater than $5\text{--}6 \text{ m s}^{-1}$. However, it seems that there is some increase in the ratio for diameter values greater than $6 \mu\text{m}$, which is in agreement with the conclusion of Gerber et al. (1999). For diameters lower than $6 \mu\text{m}$, an important dispersion of points is observed that should confirm the idea that potential turbulent flow in the inlet can sweep the smallest particles and so can alter the measurements.

Thus, a relative good agreement between the inertial concentration effect showed by Gerber et al. (1999) and our results is observed. As a consequence, we have indications which tend to show that the FSSP measurements with a wind speed too low have to be removed if the variations do not correlate with data of others instruments.

5 Conclusions

Accurate measurements of cloud microphysics properties are crucial for a better understanding of cloud processes and its impact on the climate. A large set of various cloud instrumentation were developed since the 80's. However, accurate comparisons between instruments are still scarce, in particular comparisons between ground-based and airborne conditions. To address this problem, we analyzed the results of both ground-based and wind tunnel measurements performed with various instrumentations during the ROSEA campaign at the station of the Puy-de-Dôme (Central France, 1465 m altitude) in May 2013. This instrumental intercomparison includes a FSSP, a Fog Monitor 100, a PWD, a PVM-100 used during ground-based conditions and two CDPs and a SPP-100 used in the wind tunnel.

Our results show very good correlations between the measurements performed by the different instruments, especially, for the shape of the size distribution and the effective-diameter values. Whereas effective diameter absolute values show good agreement within the 10 % average instrument uncertainty, total-concentration values can diverge up to a factor of 5. This result was expected in our study since there was no preliminary calibration of total particle number for the instruments we used. However, comparisons between ground-based and controlled wind measurements show good correlations, but with the same problem of the concentration-values bias. We thus propose to standardize with a reliable instrument, which does not use a sample volume. The data were thus normalized based on the bulk extinction coefficient measurements performed by the PWD. When comparing the extinction with the PWD, the results show that the measurements do not depend on the air speed of the instruments in the wind

Cloud-microphysical sensors intercomparison at the Puy-de-Dôme Observatory, France

G. Guyot et al.

Title Page

Abstract

Introduction

Conclusions

References

Tables

Figures



Back

Close

Full Screen / Esc

Printer-friendly Version

Interactive Discussion



Cloud-microphysical sensors intercomparison at the Puy-de-Dôme Observatory, France

G. Guyot et al.

Title Page

Abstract

Introduction

Conclusions

References

Tables

Figures

◀

▶

◀

▶

Back

Close

Full Screen / Esc

Printer-friendly Version

Interactive Discussion

tunnel or for ground based instruments. Moreover, the measurements can be standardized with a simple relation of proportionality, with a coefficient comprised between 0.43 and 2.2, which is valid for the entire campaign. However this is not applicable to the ground based FSSP measurements which were shown to be very sensitive to the wind speed and direction. Indeed, these measurements are highly variable when the wind speed was lower than the theoretical air speed through the inlet. The overestimation of extinction measured by the FSSP, compared to the PWD, showed some agreements with the Gerber et al. (1999) study, which highlights the inertial concentration effects. Moreover, additional orientation experiments were performed. The FSSP and FM orientation was modified with an angle ranging from 30° to 90° angle with wind speeds from 3 to 7 ms⁻¹. The results show that the induced number concentration loss is between 29 and 98 % for the FSSP and between 15 and 68 % for the FM-100. This study revealed that it is necessary to be very critical with cloud measurements when the wind speed is lower than 3 ms⁻¹ and when the angle between the wind direction and the orientation of the instruments is greater than 30°.

Finally the high dispersion of the ground based FSSP measurements compared to the others instruments is explained as follows. The transit speed of droplets in the FSSP sampling volume was investigated using the SPP measurements on the mast. The ground based SPP observations showed a strong variability in the transit speed of the cloud droplets. This variability did not depend on the variations of the pump aspiration or the wind speed. As this effect was more pronounced for small particles, the presence of turbulent flow inside the FSSP inlet could be a plausible explanation of the discrepancies of the measurements based on particle counting.

Acknowledgements. This work was performed within the framework ROSEA (Réseau d'Observatoires pour la Surveillance et l'Exploration de l'Atmosphère) and ACTRIS (Aerosols, Clouds and Trace gases Research Infra Structure Network). It was also supported by the French ANR CLIMSLIP. The authors thank the OPGC (Observatoire de Physique du Globe de Clermont) for monitoring the PdD station and Evelyn J. Freney for her help in improving the manuscript.

References

- Albrecht, B. A.: Aerosols, cloud microphysics, and fractional cloudiness, *Science*, 245, 1227–1230, 1989.
- Asmi, E., Freney, E., Hervo, M., Picard, D., Rose, C., Colomb, A., and Sellegri, K.: Aerosol cloud activation in summer and winter at puy-de-Dôme high altitude site in France, *Atmos. Chem. Phys.*, 12, 11589–11607, doi:10.5194/acp-12-11589-2012, 2012.
- Bain, M. and Gayet, J. F.: Contribution to the modeling of the ice accretion process: ice density variation with the impacted surface angle, *Ann. Glaciol.*, 4, 19–23, 1983.
- Baumgardner, D.: An analysis and comparison of five water droplet measuring instruments, *J. Appl. Meteorol.*, 22, 891–910, 1983.
- Baumgardner, D. and Spowart, M.: Evaluation of forward spectrometer probe. Part III: Time response and laser Inhomogeneity limitations, *J. Atmos. Ocean. Tech.*, 7, 666–672, 1990.
- Baumgardner, D., Strapp, W., and Dye, J. E.: Evaluation of the forward spectrometer probe. Part II: Corrections for coincidence and dead time losses, *J. Atmos. Ocean. Tech.*, 2, 626–632, 1985.
- Baumgardner, D., Brenguier, J., Bucholtz, A., Coe, H., DeMott, P., Garrett, T., Gayet, J., Hermann, M., Heymsfield, A., Korolev, A., Krämer, M., Petzold, A., Strapp, W., Pilewskie, P., Taylor, J., Twohy, C., Wendisch, M., Bachalo, W., and Chuang, P.: Airborne instruments to measure atmospheric aerosol particles, clouds and radiation: a cook's tour of mature and emerging technology, *Atmos. Res.*, 102, 10–29, doi:10.1016/j.atmosres.2011.06.021, 2011.
- Bennartz, R., Shupe, M. D., Turner, D., Walden, V. P., Steffen, K., Cox, C. J., Kulie, M. S., Miller, N. B., and Pettersen, C.: July 2012 Greenland melt extent enhanced by low-level liquid clouds, *Nature*, 496, 83–86, doi:10.1038/nature12002, 2013.
- Boucher, O., Randall, D., Artaxo, P., Bretherton, C., Feingold, G., Forster, P., Kerminen, V.-M., Kondo, Y., Liao, H., Lohmann, U., Rasch, P., Satheesh, S. K., Sherwood, S., Stevens, B., and Zhang, X. Y.: Clouds and aerosols, in: *Climate Change 2013: The Physical Science Basis. Contribution of Working Group I to the Fifth Assessment Report of the Intergovernmental Panel on Climate Change*, Cambridge University Press, Cambridge, UK and New York, NY, USA, 2013.
- Boulon, J., Sellegri, K., Hervo, M., Picard, D., Pichon, J.-M., Fréville, P., and Laj, P.: Investigation of nucleation events vertical extent: a long term study at two different altitude sites, *Atmos. Chem. Phys.*, 11, 5625–5639, doi:10.5194/acp-11-5625-2011, 2011.

Cloud-microphysical sensors intercomparison at the Puy-de-Dôme Observatory, France

G. Guyot et al.

Title Page

Abstract

Introduction

Conclusions

References

Tables

Figures

◀

▶

◀

▶

Back

Close

Full Screen / Esc

Printer-friendly Version

Interactive Discussion



Cloud-microphysical sensors intercomparison at the Puy-de-Dôme Observatory, France

G. Guyot et al.

Title Page

Abstract

Introduction

Conclusions

References

Tables

Figures

◀

▶

◀

▶

Back

Close

Full Screen / Esc

Printer-friendly Version

Interactive Discussion

- Bourcier, L., Sellegri, K., Chausse, P., Pichon, J. M., and Laj, P.: Seasonal variation of water-soluble inorganic components in aerosol size-segregated at the puy de Dôme station (1465 m a.s.l.), France, *J. Atmos. Chem.*, 69, 47–66, doi:10.1007/s10874-012-9229-2, 2012.
- Brenguier, J. L., Pawlowska, H., and Schüller, L.: Cloud microphysical and radiative properties for parameterization and satellite monitoring of the indirect effect of aerosol on climate, *J. Geophys. Res.*, 108, 8632, doi:10.1029/2002JD002682, 2003.
- Brenguier, J.-L., Burnet, F., and Geoffroy, O.: Cloud optical thickness and liquid water path – does the k coefficient vary with droplet concentration?, *Atmos. Chem. Phys.*, 11, 9771–9786, doi:10.5194/acp-11-9771-2011, 2011.
- Brenguier, J.-L., Bachalo, W. D., Chuang, P. Y., Esposito, B. M., Fugal, J., Garrett, T., Gayet, J.-F., Gerber, H., Heymsfield, A., Kokhanovsky, A., Korolev, A., Lawson, R. P., Rogers, D. C., Shaw, R. A., Strapp, W., and Wendisch, M.: In situ measurements of cloud and precipitation particles, in: *Airborne Measurements for Environmental Research: Methods and Instruments*, edited by: Wendisch, M. and Brenguier, J.-L., Wiley-VCH Verlag GmbH & Co. KGaA, Weinheim, Germany, doi:10.1002/9783527653218.ch5, 2013.
- Burnet, F. and Brenguier, J. L.: Validation of droplet spectra and liquid water content measurements, *Phys. Chem. Earth B*, 24, 249–254, 1999.
- Burnet, F. and Brenguier, J. L.: Comparison between standard and modified Forward Scattering Spectrometer Probes during the Small Cumulus Microphysics Study, *J. Atmos. Ocean. Tech.*, 19, 1516–1531, 2002.
- Cerni, T.: Determination of the size and concentration of cloud drops with an FSSP, *J. Clim. Appl. Meteorol.*, 22, 1346–1355, 1983.
- Choularton, T. W., Consterdine, I. E., Gardiner, B. A., Gay, M. J., Hill, M. K., Latham, J., and Stromberg, M.: Field studies of the optical and microphysical characteristics of clouds enveloping Great Dun Fell, *Q. J. Roy Meteor. Soc.*, 112, 131–148, 1986.
- Deguillaume, L., Charbouillot, T., Joly, M., Vaïtilingom, M., Parazols, M., Marinoni, A., Amato, P., Delort, A.-M., Vinatier, V., Flossmann, A., Chaumerliac, N., Pichon, J. M., Houdier, S., Laj, P., Sellegri, K., Colomb, A., Brigante, M., and Mailhot, G.: Classification of clouds sampled at the puy de Dôme (France) based on 10 yr of monitoring of their physicochemical properties, *Atmos. Chem. Phys.*, 14, 1485–1506, doi:10.5194/acp-14-1485-2014, 2014.
- Droplet Measurement Technologies: Fog Monitor Model FM-100 Operator Manual (DOC-0088 Revision H), published by Droplet Measurement Technologies, Inc., Boulder, USA, 2011.

**Cloud-microphysical
sensors
intercomparison at
the Puy-de-Dôme
Observatory, France**

G. Guyot et al.

Title Page

Abstract

Introduction

Conclusions

References

Tables

Figures

◀

▶

◀

▶

Back

Close

Full Screen / Esc

Printer-friendly Version

Interactive Discussion



Kamphus, M., Ettner-Mahl, M., Klimach, T., Drewnick, F., Keller, L., Cziczo, D. J., Mertes, S., Borrmann, S., and Curtius, J.: Chemical composition of ambient aerosol, ice residues and cloud droplet residues in mixed-phase clouds: single particle analysis during the Cloud and Aerosol Characterization Experiment (CLACE 6), *Atmos. Chem. Phys.*, 10, 8077–8095, doi:10.5194/acp-10-8077-2010, 2010.

Kenneth, V. and Ochs, H.: Warm-rain initiation: an overview of microphysical mechanisms, *J. Appl. Meteorol.*, 32, 608–625, 1993.

Knollenberg, R. G.: Practical applications of low power lasers, *SPIE*, 92, 137–152, 1976.

Knollenberg, R. G.: Techniques for probing cloud microstructure, in: *Clouds, their Formation, Optical Properties and Effects*, edited by: Hobbs, P. V. and Deepak, A., Academic Press, New York, USA, 15–92, 1981.

Lance, S., Brock, C. A., Rogers, D., and Gordon, J. A.: Water droplet calibration of the Cloud Droplet Probe (CDP) and in-flight performance in liquid, ice and mixed-phase clouds during ARCPAC, *Atmos. Meas. Tech.*, 3, 1683–1706, doi:10.5194/amt-3-1683-2010, 2010.

Marinoni, A., Laj, P., Sellegri, K., and Mailhot, G.: Cloud chemistry at the Puy de Dôme: variability and relationships with environmental factors, *Atmos. Chem. Phys.*, 4, 715–728, doi:10.5194/acp-4-715-2004, 2004.

McFarquhar, G., Ghan, S. J., Verlinde, J., Korolev, A., Strapp, J. W., Schmid, B., Tomlinson, J., Wolde, M., Brooks, S., Cziczo, D., Dubey, M., Fan, J., Flynn, C., Gultepe, I., Hubbe, J., Gilles, M., Laskin, A., Lawson, P., Leaitch, W., Liu, P., Liu, X., Lubin, D., Mazzoleni, C., Mac Donald, A.M., Moffet, R., Morrison, H., Ovchinnikov, M., Shupe, M., Turner, D., Xie, S., Zelenyuk, A., Bae, K., Freer, M., and Glen, A.: Indirect and semi-direct aerosol campaign: the impact of Arctic aerosols on clouds, *B. Am. Meteorol. Soc.*, 92, 183–201, doi:10.1175/2010BAMS2935.1, 2011.

Mertes, S., Schwarzenböck, A., Laj, P., Wobrock, W., Pichon, J. M., Orsi, G., and Heintzenberg, J.: Changes of cloud microphysical properties during the transition from supercooled to mixed-phase conditions during CIME, *Atmos. Res.*, 58, 267–294, 2001.

Mie, G.: Beiträge zur Optik trüber Medien, speziell kolloidaler Metallösungen, *Ann. Phys.-Berlin*, 330, 377–445, 1908.

Petters, J. L., Harrington, J. Y., and Clothiaux, E.: Radiative-dynamical feedbacks in low liquid water path stratiform clouds, *J. Atmos. Sci.*, 69, 1498–1512, doi:10.1175/JAS-D-11-0169.1, 2012.

overview and modeling of the microphysical processes during the seeding by isentropic gas expansion, Atmos. Res., 58, 231–265, 2001.

AMTD

8, 5511–5563, 2015

Cloud-microphysical sensors intercomparison at the Puy-de-Dôme Observatory, France

G. Guyot et al.

Title Page

Abstract

Introduction

Conclusions

References

Tables

Figures



Back

Close

Full Screen / Esc

Printer-friendly Version

Interactive Discussion



Cloud-microphysical sensors intercomparison at the Puy-de-Dôme Observatory, France

G. Guyot et al.

Table 1. Data availability for each instrument used during ROSEA.

Date	Wind tunnel				Roof				meteo
	SPP	CDP 1	CDP 2	FSSP	PVM 1	PVM 2	PWD	FM 100	
16 May 2013	✓	✓	✓	✓	×	✓	✓	✓	cloudy
17 May 2013	×	×	×	✓	✓	×	✓	✓	cloudy
19 May 2013	×	×	×	✓	✓	×	✓	✓	cloudy
20 May 2013	×	×	×	✓	✓	×	✓	✓	cloudy
21 May 2013	×	×	×	✓	×	×	✓	✓	cloudy
22 May 2013	✓	✓	×	✓	×	×	✓	✓	cloudy
23 May 2013	×	×	×	×	~	~	✓	✓	cloudy
24 May 2013	✓	✓	×	×	×	✓	✓	✓	cloudy
25 May 2013	×	×	×	×	✓	✓	✓	✓	cloudy
26 May 2013	×	×	×	×	✓	✓	✓	✓	cloudy
27 May 2013	×	×	×	✓	✓	✓	✓	✓	clear
28 May 2013	✓	✓	×	✓	✓	✓	✓	✓	cloudy

✓ = Data available.

~ = Data available during a part of the day.

× = Data not available.

Title Page

Abstract

Introduction

Conclusions

References

Tables

Figures

◀

▶

◀

▶

Back

Close

Full Screen / Esc

Printer-friendly Version

Interactive Discussion



Cloud-microphysical sensors intercomparison at the Puy-de-Dôme Observatory, France

G. Guyot et al.

Table 2. Instrumental set-up during the ROSEA intercomparison campaign at the Puy-de-Dôme.

Instrument	Measured parameter(s)	Measurement range	Accuracy	Time resolution
Forward Scattering Spectrometer Probe (FSSP and SPP)	size distribution	2–47 μm	D: $\pm 3 \mu\text{m}$ Number conc: $\pm 20 \%$	1 s
Fog Monitor (FM)	size distribution	2–50 μm	D: $\pm 3 \mu\text{m}$ Number conc: $\pm 100 \%$	1 s
Cloud Droplet Probe (CDP)	size distribution	2–50 μm	D: $\pm 3 \mu\text{m}$ Number conc: $\pm 50 \%$	1 s
Particle Volume Monitor (PVM)	extinction, LWC, Reff	3–45 μm	LWC: $\pm 10 \%$	PVM1: 5 min PVM2: 1 s
Present Weather Detector (PWD 22)	extinction	all	$\pm 10 \%$	1 min

Title Page

Abstract

Introduction

Conclusions

References

Tables

Figures

◀

▶

◀

▶

Back

Close

Full Screen / Esc

Printer-friendly Version

Interactive Discussion

Cloud-microphysical sensors intercomparison at the Puy-de-Dôme Observatory, France

G. Guyot et al.

Table 3. Summary of the cloud extinction coefficient intercomparison performed during ROSEA. The coefficient a is the slope of the linear regression, the correlation coefficient R^2 is also indicated. The bolded part corresponds to the standardization of each instrument according to the PWD, the values of a give the factor of standardization.

	FM 100	Roof PVM1	FSSP	SPP	Wind tunnel CDP1	CDP2
PWD	$a = 2.23$; $R^2 = 0.58$	$a = 1.17$; $R^2 = 0.86$	$a = 0.35$; $R^2 = 0.24$	$a = 0.44$; $R^2 = 0.86$	$a = 0.63$; $R^2 = 0.72$	$a = 1.05$; $R^2 = 0.72$
FM 100		$a = 0.45$; $R^2 = 0.74$	$a = 0.15$; $R^2 = 0.79$	$a = 0.26$; $R^2 = 0.61$	$a = 0.39$; $R^2 = 0.61$	$a = 0.46$; $R^2 = 0.61$
PVM1			$a = 0.34$; $R^2 = 0.64$	/	/	/
FSSP				no correlation	no correlation	no correlation
SPP					$a = 0.69$; $R^2 = 0.95$	$a = 0.42$; $R^2 = 0.91$
CDP1						$a = 0.59$; $R^2 = 0.91$
CDP2						

Title Page

Abstract

Introduction

Conclusions

References

Tables

Figures

◀

▶

◀

▶

Back

Close

Full Screen / Esc

Printer-friendly Version

Interactive Discussion

Cloud-microphysical sensors intercomparison at the Puy-de-Dôme Observatory, France

G. Guyot et al.

Table 4. FSSP concentration loss in percentage compared to the isoaxial measurement concentration, as a function of the wind speed and the angle between wind direction and instrument orientation. For each angles and wind speed values, this percentage is computed for the entire size range (2 to 45 μm), the small particles (2 to 14 μm) and the large particles (14 to 29 μm).

	wind	3 ms ⁻¹	5 ms ⁻¹	6 ms ⁻¹	7 ms ⁻¹
30°	total	29	74	75	28
	2 to 14 μm	31	58	68	30
	14 to 29 μm	25	94	86	26
60°	total	71	88	95	93
	2 to 14 μm	65	82	93	87
	14 to 29 μm	80	96	99	99
90°	total	46	95	96	98
	2 to 14 μm	41	93	95	97
	14 to 29 μm	55	97	99	100

Title Page

Abstract

Introduction

Conclusions

References

Tables

Figures

◀

▶

◀

▶

Back

Close

Full Screen / Esc

Printer-friendly Version

Interactive Discussion

Cloud-microphysical sensors intercomparison at the Puy-de-Dôme Observatory, France

G. Guyot et al.

Table 5. Same as Table 4, for the FM 100.

	wind	3 ms^{-1}	5 ms^{-1}	6 ms^{-1}	7 ms^{-1}
30°	total	15	43	34	21
	2 to 14 μm	16	32	34	21
	14 to 29 μm	18	74	35	31
60°	total	45	55	68	62
	2 to 14 μm	41	44	67	50
	14 to 29 μm	62	84	71	90
90°	total	37	58	47	54
	2 to 14 μm	33	59	52	52
	14 to 29 μm	49	67	16	52

Title Page

Abstract

Introduction

Conclusions

References

Tables

Figures

◀

▶

◀

▶

Back

Close

Full Screen / Esc

Printer-friendly Version

Interactive Discussion

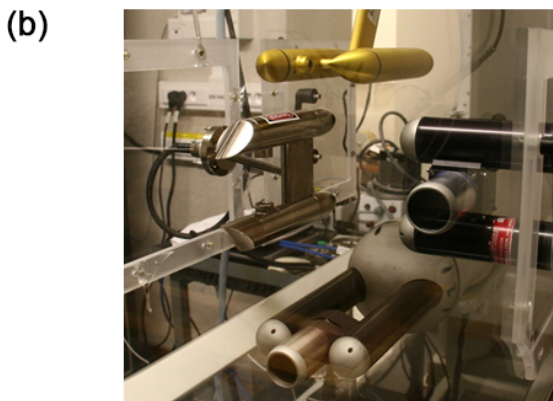
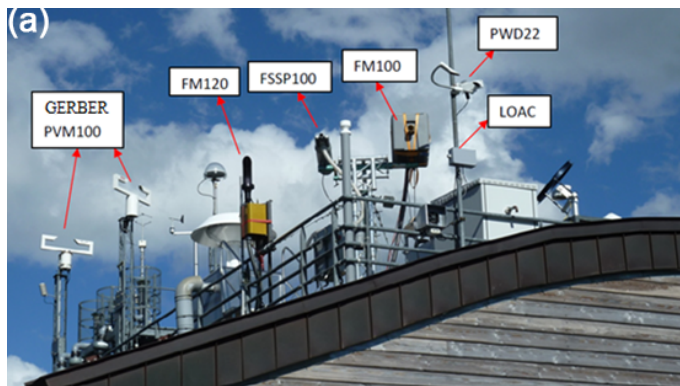


Figure 1. (a) Instruments set-up on the roof. The FSSP and the FM 100 were placed on the mast, which can be oriented manually, so the direction where pointed these two instruments can be chosen and (b) instruments set-up in the wind tunnel, the SPP at the right, the CDP 1 at the top and the CDP 2 at the left.

Cloud-microphysical sensors intercomparison at the Puy-de-Dôme Observatory, France

G. Guyot et al.

Title Page

Abstract

Introduction

Conclusions

References

Tables

Figures

◀

▶

◀

▶

Back

Close

Full Screen / Esc

Printer-friendly Version

Interactive Discussion



Cloud-microphysical sensors intercomparison at the Puy-de-Dôme Observatory, France

G. Guyot et al.

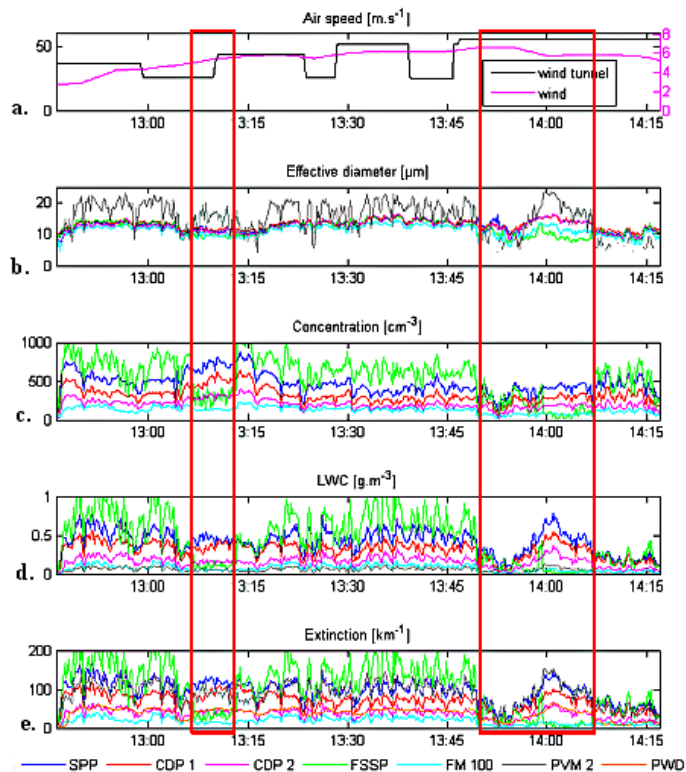


Figure 2. Time series of the 16 May experiment of the main measured parameters: **(a)** ambient wind speed (purple) and wind tunnel air speed (black); **(b)** effective diameter; **(c)** concentration; **(d)** LWC and **(e)** extinction. The data are 10 s averaged, except for the PWD measurements performed with a 1 min time resolution. The red-framed parts of the time series correspond to additional experiments where the orientation of the instruments on the mast was changed (for the FM 100 and the FSSP).

[Title Page](#)
[Abstract](#)
[Introduction](#)
[Conclusions](#)
[References](#)
[Tables](#)
[Figures](#)
[◀](#)
[▶](#)
[◀](#)
[▶](#)
[Back](#)
[Close](#)
[Full Screen / Esc](#)
[Printer-friendly Version](#)
[Interactive Discussion](#)

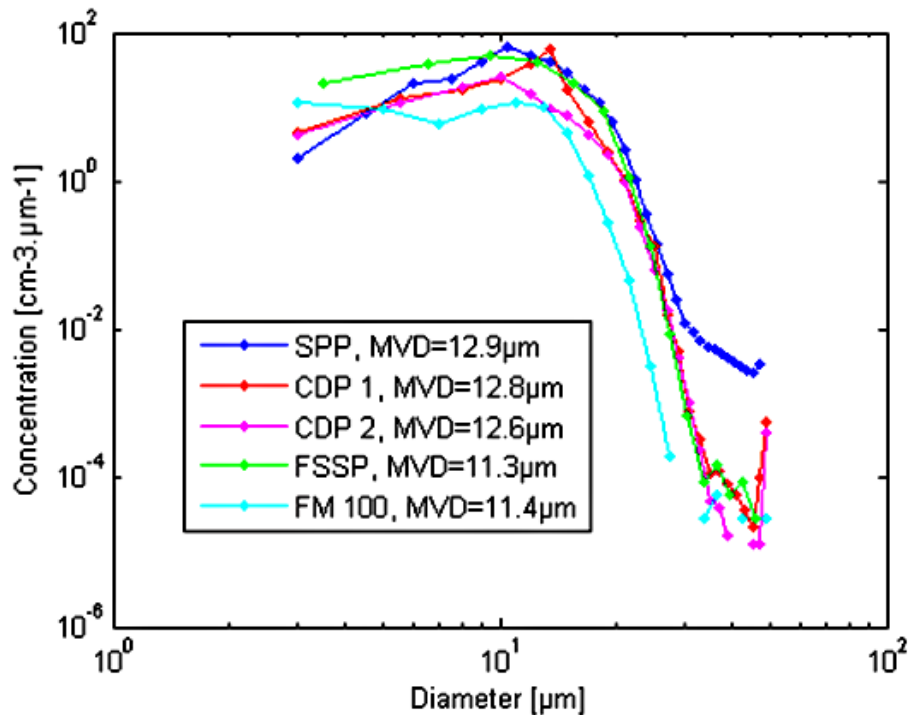


Figure 3. Averaged size distribution for the 16 May over the period of time shown in Fig. 2 (i.e. 12:46 p.m. to 2.17 p.m.). The color corresponds to the different instruments displayed in the legend. The average median volume diameter MVD is also shown.

Cloud-microphysical sensors intercomparison at the Puy-de-Dôme Observatory, France

G. Guyot et al.

Title Page	
Abstract	Introduction
Conclusions	References
Tables	Figures
◀	▶
◀	▶
Back	Close
Full Screen / Esc	
Printer-friendly Version	
Interactive Discussion	



Cloud-microphysical sensors intercomparison at the Puy-de-Dôme Observatory, France

G. Guyot et al.

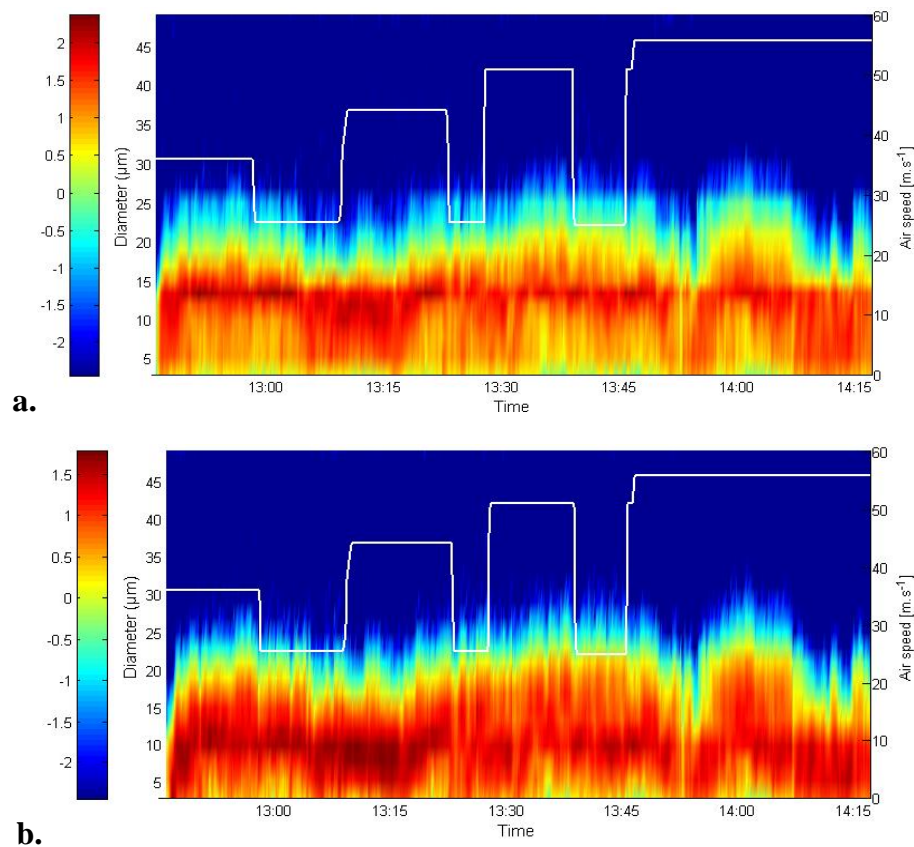


Figure 4. Time series of the 10 s average size distributions of CDP1 (a) and CDP2 (b), for the 16 May. The logarithmic values of the concentration for each size bin of the CDP in cm⁻³ μm⁻¹ are color-coded. The air speed applied in the wind tunnel is plotted in white.

Title Page

Abstract

Introduction

Conclusions

References

Tables

Figures

◀

▶

◀

▶

Back

Close

Full Screen / Esc

Printer-friendly Version

Interactive Discussion

Cloud-microphysical sensors intercomparison at the Puy-de-Dôme Observatory, France

G. Guyot et al.

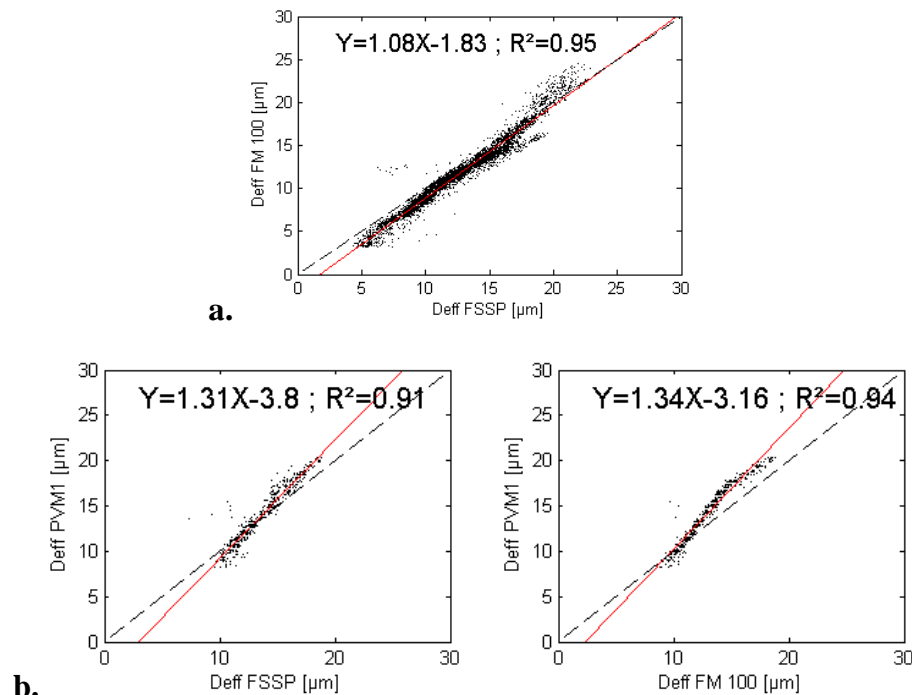


Figure 5. (a) Comparison between the 1 min averaged effective diameters of the FM 100 and the FSSP. (b) Comparison between the 5 min averaged effective diameters between the PVM1 and the FSSP (left) and with the FM 100 (right).

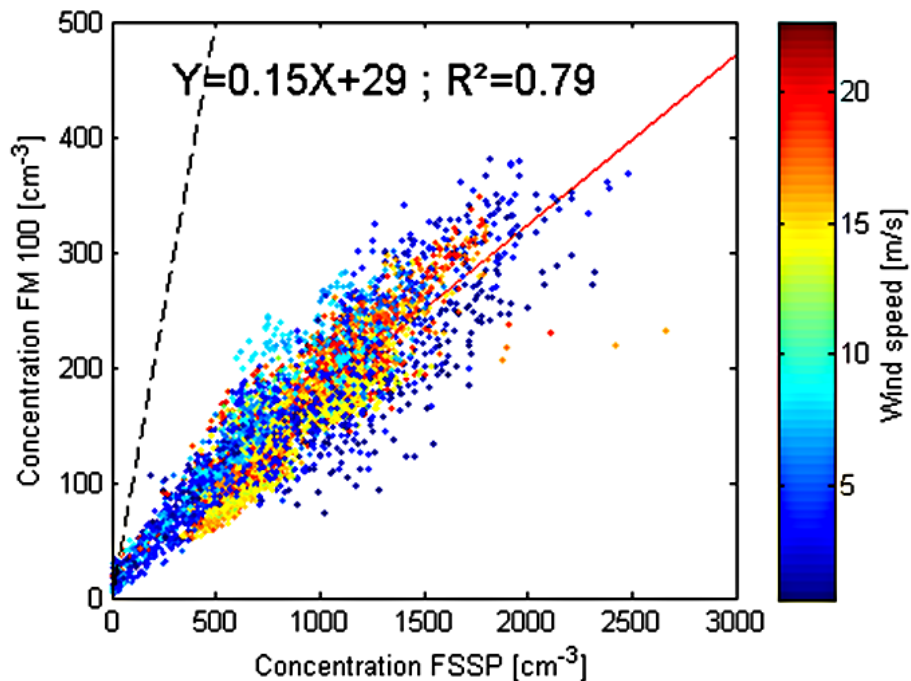


Figure 6. 1 min averaged concentration in cm⁻³ measurements obtained from the FM 100 as a function of the FSSP concentration of the FSSP. The color shows the values of the wind speed.

**Cloud-microphysical
sensors
intercomparison at
the Puy-de-Dôme
Observatory, France**

G. Guyot et al.

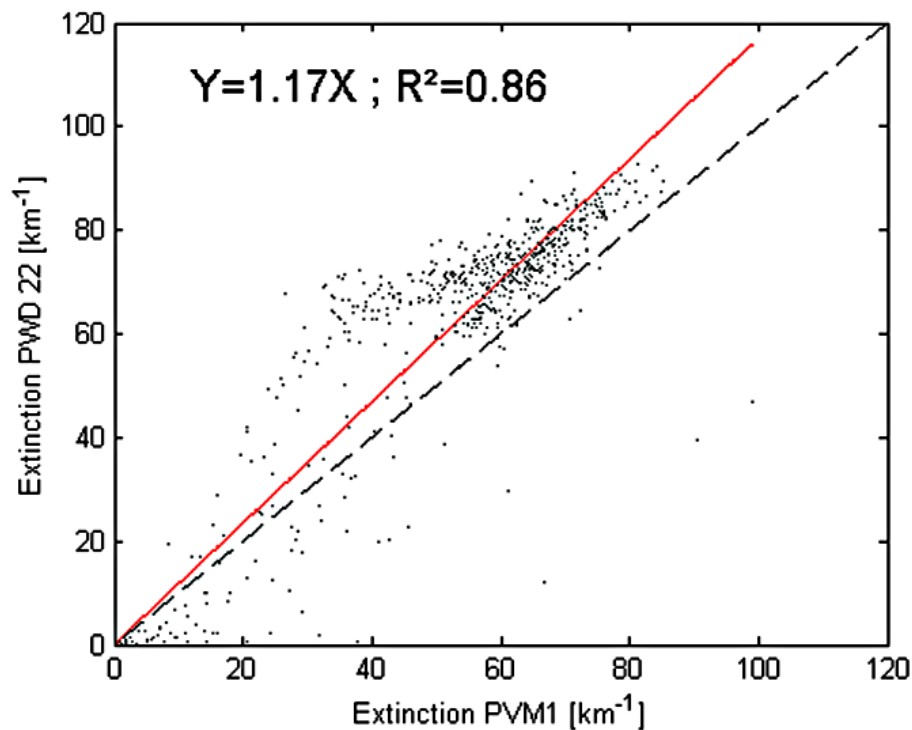


Figure 7. Scatter plot of the PWD and PVM1 5 min average extinction coefficients.

[Title Page](#)[Abstract](#)[Introduction](#)[Conclusions](#)[References](#)[Tables](#)[Figures](#)[◀](#)[▶](#)[◀](#)[▶](#)[Back](#)[Close](#)[Full Screen / Esc](#)[Printer-friendly Version](#)[Interactive Discussion](#)

Cloud-microphysical sensors intercomparison at the Puy-de-Dôme Observatory, France

G. Guyot et al.

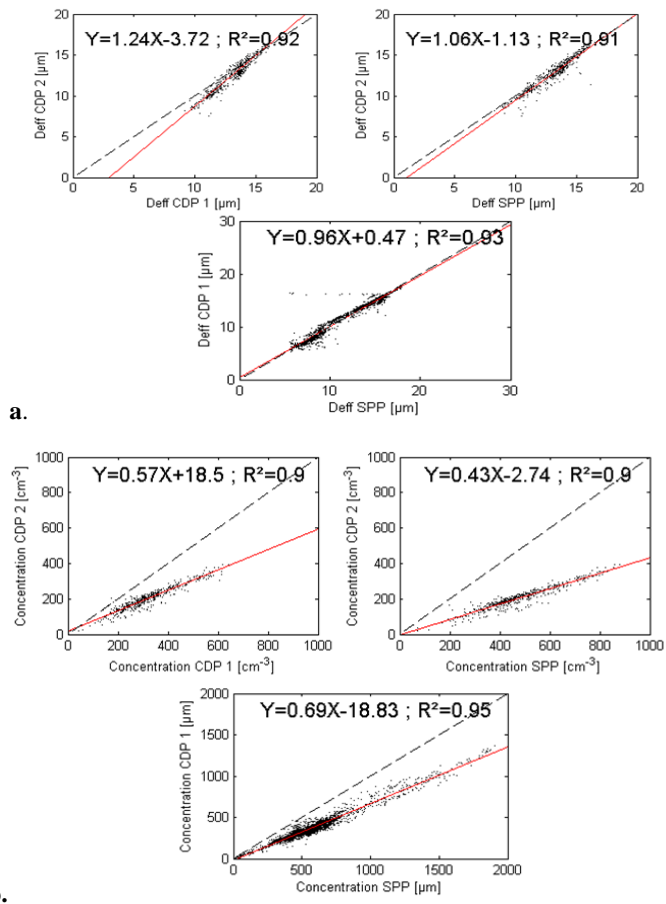


Figure 8. (a) 10 s averaged data comparison of the effective diameter measured by the instruments installed in the wind tunnel, i.e. the CDP1, the CDP2 and the SPP; and (b) 10 s averaged data comparison of the concentration measured by the instruments installed in the wind tunnel.

Title Page

Abstract

Introduction

Conclusions

References

Tables

Figures

◀

▶

◀

▶

Back

Close

Full Screen / Esc

Printer-friendly Version

Interactive Discussion

Cloud-microphysical sensors intercomparison at the Puy-de-Dôme Observatory, France

G. Guyot et al.

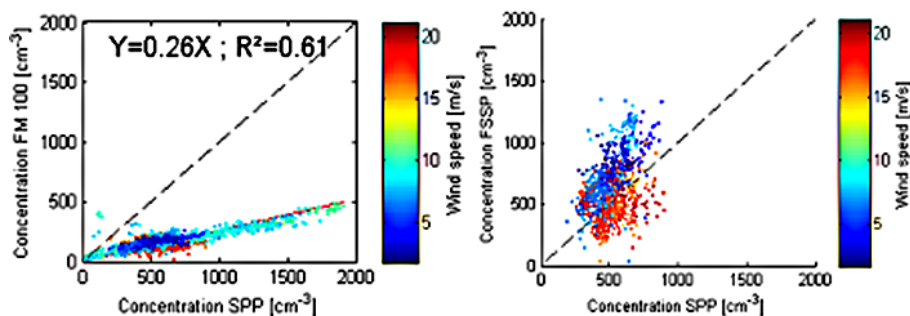


Figure 9. Scatter plots of the 10 s averaged concentrations measured by the FM 100 (left) and the FSSP (right), in ambient conditions, with the wind tunnel SPP. The color reveals the ambient wind speed.

[Title Page](#)[Abstract](#)[Introduction](#)[Conclusions](#)[References](#)[Tables](#)[Figures](#)[◀](#)[▶](#)[◀](#)[▶](#)[Back](#)[Close](#)[Full Screen / Esc](#)[Printer-friendly Version](#)[Interactive Discussion](#)

Cloud-microphysical sensors intercomparison at the Puy-de-Dôme Observatory, France

G. Guyot et al.

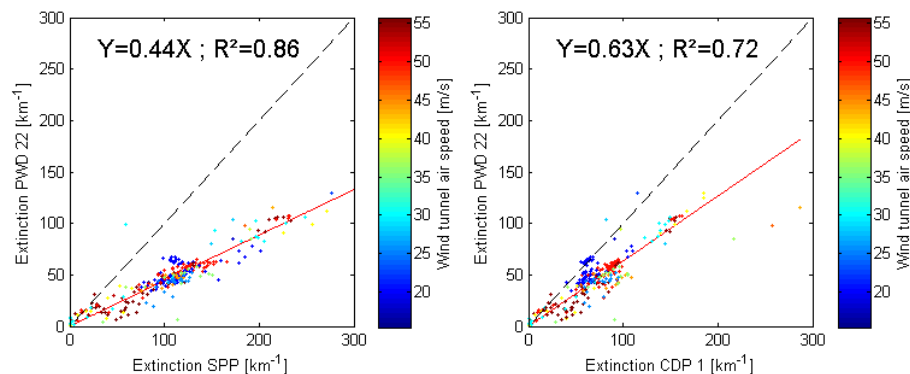


Figure 10. 1 min averaged SPP and CDP 1 extinctions compared with the PWD extinction for the four wind tunnel experiments. The air speed applied in the wind tunnel is shown on the colorbar.

[Title Page](#)[Abstract](#)[Introduction](#)[Conclusions](#)[References](#)[Tables](#)[Figures](#)[◀](#)[▶](#)[◀](#)[▶](#)[Back](#)[Close](#)[Full Screen / Esc](#)[Printer-friendly Version](#)[Interactive Discussion](#)

Cloud-microphysical sensors intercomparison at the Puy-de-Dôme Observatory, France

G. Guyot et al.

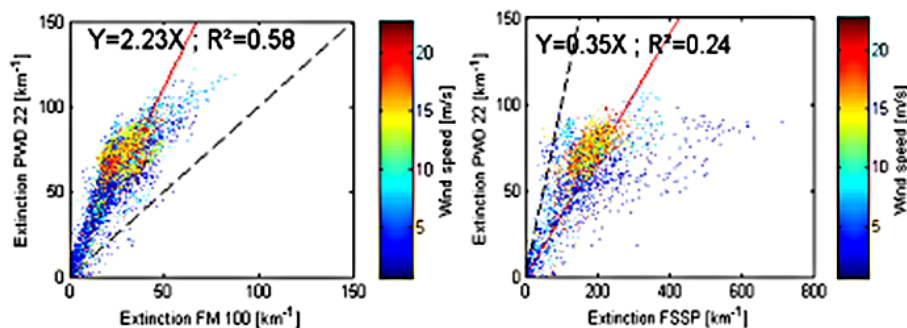


Figure 11. 1 min averaged FSSP and FM 100 extinctions vs. the PWD extinction during the entire ROSEA campaign. The measurements have been selected for cloudy events. The red line reveals the linear correlation and the colorbar shows the values of the wind speed.

[Title Page](#)[Abstract](#)[Introduction](#)[Conclusions](#)[References](#)[Tables](#)[Figures](#)[◀](#)[▶](#)[◀](#)[▶](#)[Back](#)[Close](#)[Full Screen / Esc](#)[Printer-friendly Version](#)[Interactive Discussion](#)

Cloud-microphysical sensors intercomparison at the Puy-de-Dôme Observatory, France

G. Guyot et al.

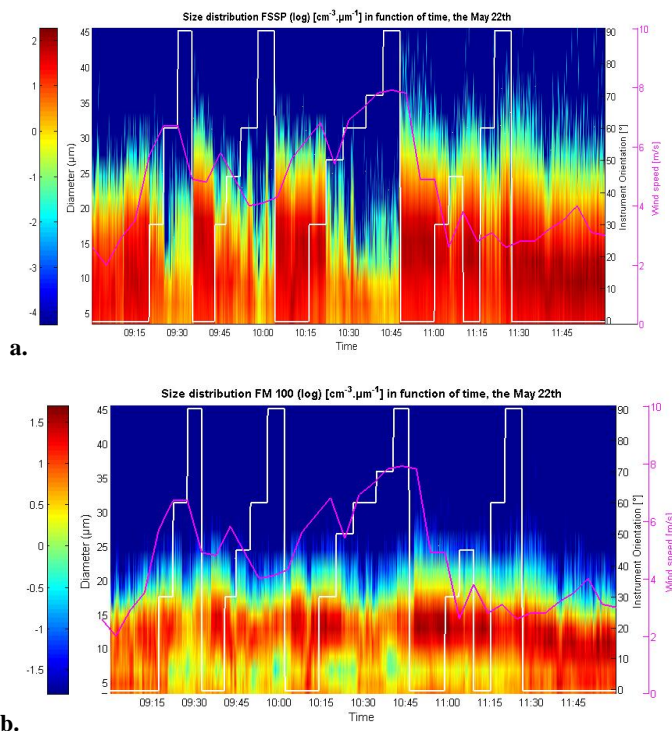


Figure 12. FSSP (a) and FM 100 (b) time series of the size distribution [cm⁻³ μm⁻¹] during the 22 May. The angle between the wind direction and the mast direction is plotted in white and the wind speed in magenta.

Cloud-microphysical sensors intercomparison at the Puy-de-Dôme Observatory, France

G. Guyot et al.

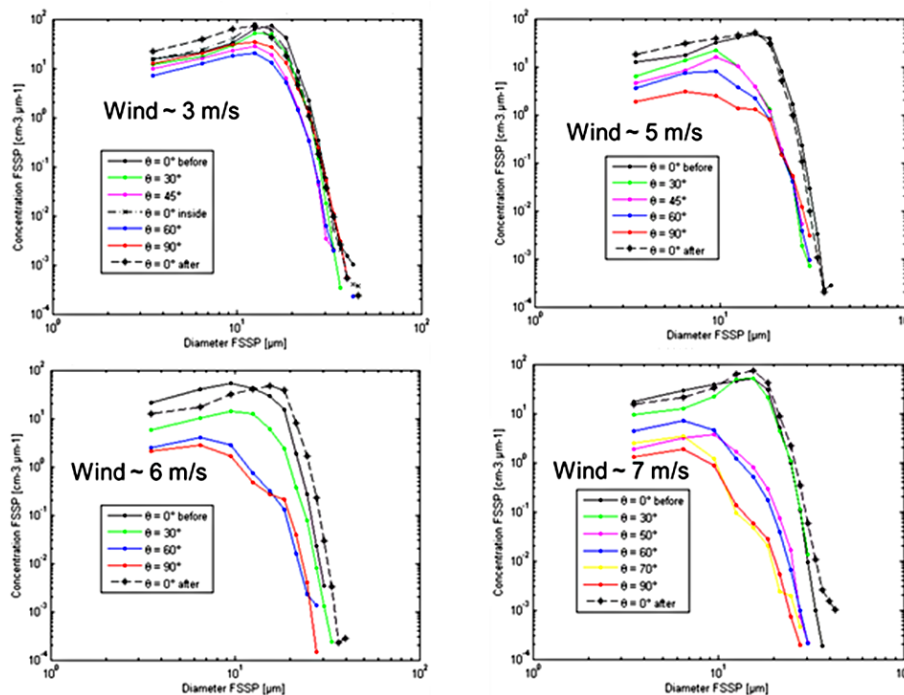


Figure 13. FSSP size distribution averaged for each angle θ corresponding to the angle between the wind direction and the instrument orientation, for the four manipulations. The averaged wind speed is indicated for each experiment.

[Title Page](#)
[Abstract](#)
[Introduction](#)
[Conclusions](#)
[References](#)
[Tables](#)
[Figures](#)
[◀](#)
[▶](#)
[◀](#)
[▶](#)
[Back](#)
[Close](#)
[Full Screen / Esc](#)
[Printer-friendly Version](#)
[Interactive Discussion](#)

**Cloud-microphysical sensors
intercomparison at
the Puy-de-Dôme
Observatory, France**

G. Guyot et al.

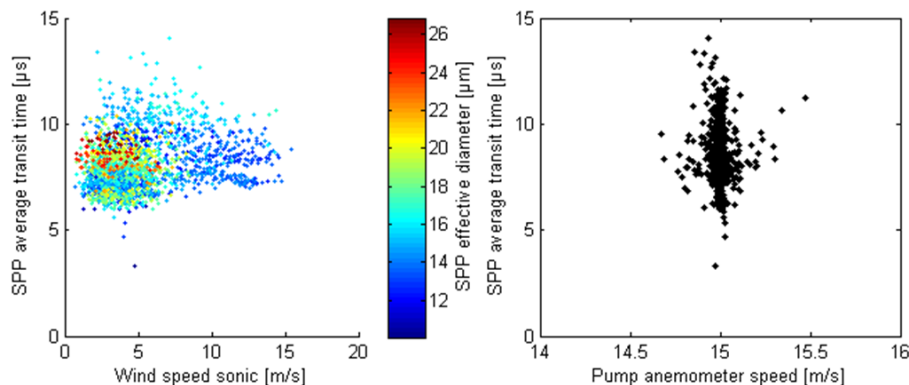


Figure 14. SPP average transit time as a function of the ambient wind speed (left) and of the pump suction speed (right). The color shows the effective diameter measured by the SPP. The data are averaged over 1 min.

Title Page

Abstract

Introduction

Conclusions

References

Tables

Figures

◀

▶

◀

▶

Back

Close

Full Screen / Esc

Printer-friendly Version

Interactive Discussion

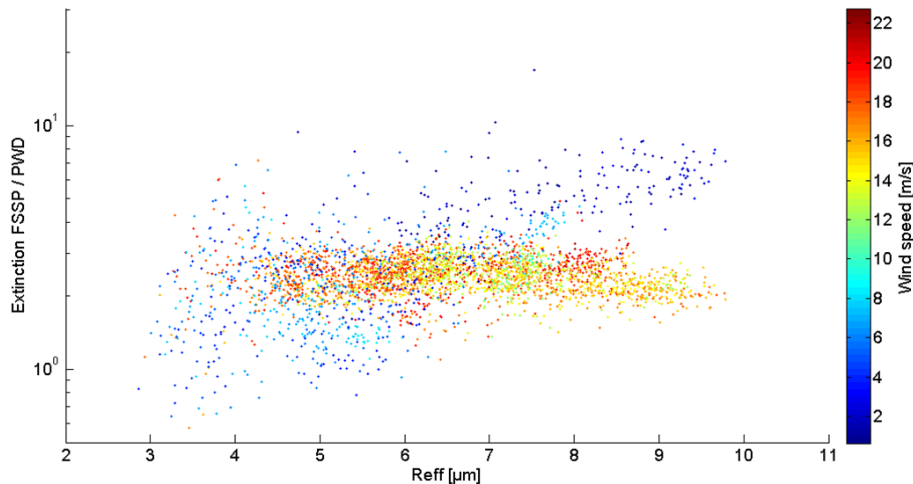


Figure 15. Extinction ratio between the FSSP and the PWD as a function of effective radius of cloud droplets and ambient wind speed, during the ROSEA campaign.

Cloud-microphysical sensors intercomparison at the Puy-de-Dôme Observatory, France

G. Guyot et al.

Title Page	
Abstract	Introduction
Conclusions	References
Tables	Figures
◀	▶
◀	▶
Back	Close
Full Screen / Esc	
Printer-friendly Version	
Interactive Discussion	

